

Adaptive Windowing for Optimal Visualization of Medical Images Based on a Structural Fidelity Measure

Hojatollah Yeganeh¹, Zhou Wang¹, and Edward R. Vrscay²

¹ Department of Electrical and Computer Engineering, Faculty of Engineering, University of Waterloo, Waterloo, Ontario, Canada N2L 3G1

² Department of Applied Mathematics, Faculty of Mathematics, University of Waterloo, Waterloo, Ontario, Canada N2L 3G1
hyeganeh@uwaterloo.ca, zhouwang@ieee.org, ervrscay@uwaterloo.ca

Abstract. Medical imaging devices often capture the raw data with high precision, producing high dynamic range (HDR) images. To visualize HDR images on regular displays, there has been an increasing number of tone mapping algorithms developed in recent years that convert HDR to low dynamic range (LDR) images. To visualize HDR medical images, a so-called “windowing” procedure is typically employed by which the structural details within the intensity region of interest is mapped to the dynamic range of regular displays. Linear mapping is the most straightforward windowing operator, but may not be the optimal mapping function in terms of structure preserving. Here we propose a framework to adaptively find the optimal windowing function for different images. Specifically, a recently developed structural fidelity measure for tone mapped images is employed to adaptively optimize the windowing function, so as to achieve the best structural fidelity with respect to the original HDR image. Experiments demonstrate the promising performance of the proposed adaptive windowing method.

1 Introduction

Medical images are typically captured and stored using formats that allocate more bits to each pixel than those assumed by standard displays. As such, they are high dynamic range (HDR) images [5]. The HDR image format provides sufficient precision for medical imaging in terms of capture, processing and rendering in medical imaging. A number of standards have been introduced to store HDR medical images: The Digital Imaging and Communications in Medicine (DICOM) is one of the most widely used standards in medical image repositories.

A problem often encountered in practice is how to visualize HDR medical images on regular displays which are designed to display low dynamic range (LDR) images. In order to overcome this problem, a number of tone mapping algorithms that convert HDR to LDR images have been developed. Many of these methods employ a straightforward windowing method which maps an intensity interval of interest linearly to the dynamic range of the display. Such intervals of

interest vary for different body parts. These intervals can be defined using two parameters: (i) window width, the range of the interval, to be denoted here as W and (ii) the window center, the center of this interval, to be denoted as C . It follows that the tone mapping algorithm maps the range of luminance values $C - \frac{1}{2}W \leq l \leq C + \frac{1}{2}W$ to the LDR range $[0, 255]$ using a linear function. The default values for window width and window center are embedded in headers of HDR medical image files. These parameters, however, are not optimized for the visualization of different body parts. In practice, radiologists often adjust the window width and window center manually so that the details for particular body regions become more visible.

Because of the reduction in dynamic range, windowing procedures inevitably cause information loss. Moreover, the linear mapping function may not be optimal in the sense of perfectly capturing structural information. As a result, it is of interest to find optimal tone mapping functions which can faithfully preserve the structural details in a window region. In order to differentiate between the performances of different tone mapping functions, it is necessary to measure the visual qualities of the resulting 8 bit mapped images. The most straightforward method to assess the quality of medical images is subjective evaluation [2] [4]. Although subjective evaluation may be extremely valuable in determining the performance of tone mapping algorithms, it is time consuming and expensive, particularly in the case of clinical images. Therefore, it is essential to employ reliable objective quality assessment methods for medical images. PSNR and MSE are the most common objective measures used to make judgements about the quality of images [3]. However, it is well known that these methods, which are based upon the L^2 distance, are not necessarily good for visual quality assessment [6]. What complicates matters further is that these methods cannot be applied directly to the tone-mapping problem, since it involves images with different dynamic ranges.

In this work, our goal is to produce tone mapping operators that are superior to the linear mappings currently employed for the purpose of visualizing HDR medical images. Our proposed approach employs two types of continuous, monotonically increasing tone-mapping functions and tunes their parameters to map the structural information within the window width onto the display dynamic range in an optimal way. The optimization task is carried out by exploiting the structural fidelity measure introduced in [8]. Our experiments confirm that the linear mapping function is not optimal in terms of the fidelity of structural information. In addition, they show that modifying the mapping function for maximal structural fidelity measure produces medical images with higher contrast and more visible details.

2 Structural Fidelity Measurement

Since the windowing function reduces the dynamic range of an image, all the information contained in an HDR medical image cannot be preserved. Human observers, particularly doctors/radiologists, may not be aware of this loss of

information. A tool to measure structural fidelity may, therefore, play an important role in assessing the quality of LDR medical images. The structural similarity index (SSIM) framework has inspired us to develop an SSIM-based structural fidelity measure [7] [8] [9]. A modified version of the original SSIM algorithm, which contains three comparison components – luminance, contrast and structure – is applied locally. Since the window mapping function alters local luminance and contrast, the direct comparison of these quantities between HDR medical images and their LDR counterparts is inappropriate. Let x and y be two local image patches extracted from the HDR and the LDR medical images, respectively. We define a local structural fidelity measure as

$$S_{\text{local}}(x, y) = \frac{2\sigma'_x\sigma'_y + C_1}{\sigma'^2_x + \sigma'^2_y + C_1} \cdot \frac{\sigma_{xy} + C_2}{\sigma_x\sigma_y + C_2}. \quad (1)$$

The second term is the same as the structure comparison component in the usual SSIM index, where σ_x , σ_y and σ_{xy} denote the local standard deviations and cross correlation between the two corresponding patches in the HDR and LDR medical images, respectively, and C_1 and C_2 are positive stability constants. The first term corresponds to a modification of the local contrast comparison of SSIM which is based on two intuitive considerations. First, the contrast differences between HDR and LDR image patches should not be penalized as long as their contrasts are both significant or both insignificant. Second, the measure should penalize the cases in which contrast is significant in one of the image patches but not in the other. A critical issue here is to quantify the significance of local contrast. To do so, we pass the local standard deviation through a nonlinear mapping function resulting in the σ' value employed in (1).

The definition of the nonlinear mapping is based on the visual sensitivity of contrast. Practically, the human visual system (HVS) does not have a fixed threshold of contrast detection, but typically follows a gradually increasing probability in observing contrast variations [1]. In psychophysics, a so-called *psychometric function* is employed to describe the detection probability of signal strength. A common model for psychometric functions is known as *Galton's ogive* [1], which determines the detection probability density of the amplitude of the sinusoidal stimulus using a cumulative normal distribution function. In [8], Galton's psychometric function was rewritten in terms of the standard deviation of the signal. As a result the mapping between σ and σ' is defined as:

$$\sigma' = \frac{1}{\sqrt{2\pi}\theta_\sigma} \int_{-\infty}^{\sigma} \exp\left[-\frac{(t - \tau_\sigma)^2}{2\theta_\sigma^2}\right] dt, \quad (2)$$

where τ_σ is the contrast threshold and $\theta_\sigma = \tau_\sigma/3$. In [8], the contrast threshold, τ_σ , is calculated for natural images using a CSF model as well as a contrast sensitivity measurement assuming a pure sinusoidal stimulus. However, since a judgement about significant and insignificant contrast details in medical images is crucial and the neglect of any important structural information might lead to grave consequences, we prefer here to set the contrast thresholds to be very

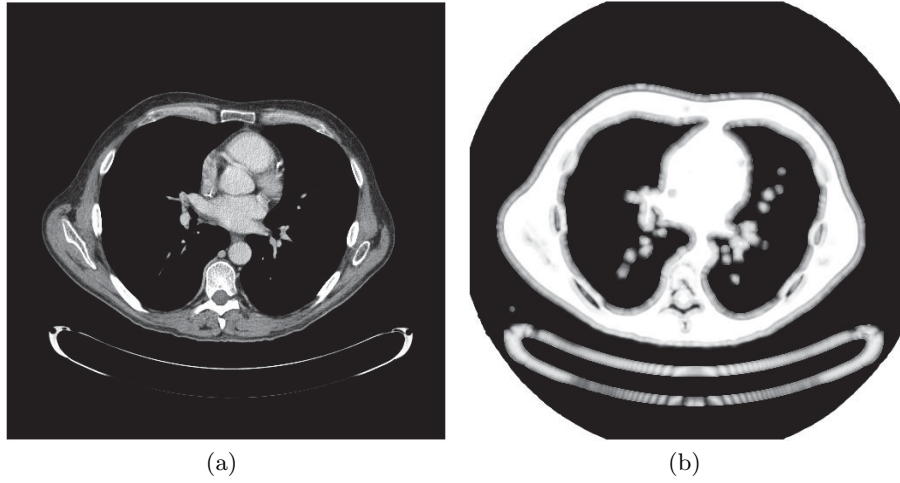


Fig. 1. Medical images which are compared with the DICOM reference file. (a) Tone mapped image using the linear mapping function $S = 0.40$. (b) Associated quality map.

small. As a result, the structural fidelity method penalizes mappings from non-flat regions to flat regions and vice-versa. In our experiments, we set τ_σ to 1 and 0.5 for HDR and LDR medical images, respectively. In (1), σ'_x and σ'_y are the mapped versions of σ_x and σ_y , respectively. They are bounded between 0 and 1, where 0 and 1 represent completely insignificant and completely significant signal strengths, respectively.

The local structural fidelity measure S_{local} is applied to an image using a sliding window that runs across the image, resulting in a map that reflects the variation of structural fidelity across space. Figure 3(a) shows a CT image of an abdomen region tone-mapped by a linear function. The quality map produced by the proposed measure is shown in Figure 3(b). The window width and window center parameters are extracted from the DICOM image header. It is interesting to observe these fidelity maps and examine how they correlate with perceived image fidelity. For example, because of the window width and window center parameters, the structural details in the lung are missing in Figure 3(a). In Figure 3(b), the quality map in the lung region is black, indicating that there are some details in the original DICOM image that are not mapped into the LDR image. On the other hand, a white region in the boundary illustrates that there is no structural information in the original DICOM image in the corners – therefore, nothing is lost by the linear mapping function. Finally, the components of the quality map are averaged to provide a single score – the overall structural fidelity-based quality measure,

$$S = \frac{1}{N} \sum_{i=1}^N S_{\text{local}}(x_i, y_i), \quad (3)$$

where x_i and y_i are the i -th patches in the HDR and LDR medical images being compared, respectively, and N is the number of patches. To implement the proposed algorithm, we set $C_1 = 0.01$, $C_2 = 10$, and employ a Gaussian sliding window of size 11×11 with standard deviation 1.5 to create the quality map.

The main advantage of the structural fidelity measure described above is the ability to comparing LDR and HDR medical images without creating an LDR image as reference. This provides a useful tool for medical imaging since radiologists do not have to produce an LDR reference image each time the window width and window center are adjusted. In contrast, commonly employed quality metrics such as PSNR and SSIM have to compare the test image with an LDR reference image generated by a windowing process. In addition, the quality map indicates the performance of tone mapping or image processing algorithms in the regions of interest. In Figure 1, the quality maps reflect the quality of heart and tissue regions regardless of the black background which is of no interest.

3 Finding the Optimal Windowing Function

Let x be the original HDR image; l_l and l_u be the lower and upper bounds of the window range, respectively; f be the windowing (or intensity mapping) function lives in the space defined by

$$\mathcal{F}_{[l_l, l_u]} = \{f : [l_l, l_u] \rightarrow [0, 1] \mid f \text{ continuous \& monotonically increasing}\}; \quad (4)$$

$T_f(\cdot)$ be the tone mapping operator that applies the function f pointwise to an image and quantize the mapped value to the dynamic range of the LDR display; and $S(\cdot, \cdot)$ be the structural fidelity measure defined in the previous section. Our goal is to search for the optimal mapping function f in terms of $S(x, T_f(x))$:

$$f_{opt} = \arg \max_{f \in \mathcal{F}_{[l_l, l_u]}} S(x, T_f(x)). \quad (5)$$

Here we consider only two subsets of this space: (i) piecewise linear functions and (ii) functions spanned by an appropriate family of sine functions.

3.1 Windowing function using piecewise linear basis

For simplicity, we consider piecewise linear functions defined by an equipartition of the HDR intensity range $[l_l, l_u]$ into n subintervals $I_k = [l_{k-1}, l_k]$ for $1 \leq k \leq K$ of length $\Delta l = (l_u - l_l)/K$. The partition points are defined by $l_k = l_l + k\Delta l$, $0 \leq k \leq n$, as such $l_l = l_0$ and $l_u = l_n$. The window width and window center are, respectively,

$$W = l_n - l_0 = n\Delta l, \quad C = \frac{1}{2}(l_0 + l_n) = l_0 + \frac{n\Delta l}{2}. \quad (6)$$

Every such equipartition piecewise linear function can be expressed as a linear combination of n basis functions. The first basis function is a “ramp” function that corresponds to a direct linear mapping in the full range:

$$\phi_0(l) = \begin{cases} (l - l_0)/W, & l_0 \leq l \leq l_n; \\ 0, & \text{otherwise.} \end{cases} \quad (7)$$

The other $n - 1$ basis functions are defined in terms of the standard triangle or “hat” function given by

$$t(l) = \begin{cases} 1 - |l|, & -1 \leq l \leq 1; \\ 0, & \text{otherwise.} \end{cases} \quad (8)$$

Specifically, we have

$$\phi_k(l) = t\left(\frac{l - l_k}{\Delta l}\right), \text{ for } k = 1, \dots, n - 1 \quad (9)$$

As such, any equipartition piecewise linear function can be expressed as

$$f(l) = \sum_{k=0}^{n-1} c_k \phi_k(l) = \phi_0(l) + \sum_{k=1}^{n-1} c_k \phi_k(l), \quad (10)$$

where the value of c_0 is known to be 1. In order for the function to be monotonically increasing, we need $0 \leq \dots \leq f(l_{k-1}) \leq f(l_k) \leq \dots \leq 1$, which yields

$$0 \leq \dots \leq c_{k-1} + \frac{k-1}{n} \leq c_k + \frac{k}{n} \leq \dots \leq 1. \quad (11)$$

For example, in the case that $n = 3$, we can derive

$$\begin{cases} c_1 \geq -\frac{1}{3}; \\ c_2 - c_1 \geq -\frac{1}{3}; \\ c_2 \geq \frac{1}{3}. \end{cases} \quad (12)$$

3.2 Windowing function using family of sine basis

The windowing function may also be expressed using a linear combination of a family of sine basis functions defined by

$$\phi_k(l) = \sin\left(\frac{k\pi(l - l_l)}{W}\right) \text{ for } l_l \leq l \leq l_u \text{ and } k = 1, 2, \dots \quad (13)$$

We then obtain an n -th order approximation of any f in $\mathcal{F}_{[l_l, l_u]}$ using the same expression as (10), where the only difference is that the triangle basis functions are replaced by the sine basis functions.

As a special case, when $n = 3$, we have

$$f(l) = \frac{l - l_l}{W} + c_1 \sin\left(\frac{\pi(l - l_l)}{W}\right) + c_2 \sin\left(\frac{2\pi(l - l_l)}{W}\right), \quad (14)$$

To ensure $f(l)$ to be monotonically increasing, its derivative needs to be no less than 0:

$$f'(l) = \frac{1}{W} + \frac{\pi c_1}{W} \cos\left(\frac{\pi(l-l_l)}{W}\right) + \frac{2\pi c_2}{W} \cos\left(\frac{2\pi(l-l_l)}{W}\right) \geq 0. \quad (15)$$

To find the extrema l^* of $f'(l)$, we set its derivative to 0, which yields

$$f''(l^*) = -\frac{\pi^2 c_1}{W^2} \sin\left(\frac{\pi(l^*-l_l)}{W}\right) - \frac{4\pi^2 c_2}{W^2} \sin\left(\frac{2\pi(l^*-l_l)}{W}\right) = 0. \quad (16)$$

Expanding the second term, we obtain

$$\sin\left(\frac{\pi(l^*-l_l)}{W}\right) \left[c_1 + 8c_2 \cos\left(\frac{\pi(l^*-l_l)}{W}\right) \right] = 0, \quad (17)$$

for which we have three possible solutions:

$$l^* = l_l, \quad (18)$$

$$l^* = l_u, \quad (19)$$

$$\cos\left(\frac{\pi(l^*-l_l)}{W}\right) = \frac{-c_1}{8c_2}. \quad (20)$$

From (20), we have

$$\cos\left(\frac{2\pi(l^*-l_l)}{W}\right) = 2\left(\frac{-c_1}{8c_2}\right)^2 - 1 = \frac{c_1^2}{32c_2^2} - 1. \quad (21)$$

Substituting (18), (19) and the pair (20) and (21) into (15), we obtain the three constraints on the solutions of c_1 and c_2 :

$$\begin{cases} c_1 + 2c_2 \geq -\frac{1}{\pi} \\ -c_1 + 2c_2 \geq -\frac{1}{\pi} \\ \frac{c_1^2}{16c_2} + 2c_2 \leq \frac{1}{\pi} \end{cases}. \quad (22)$$

3.3 Finding optimal windowing functions

With the two types of windowing functions defined in previous subsections, the problem of finding f_{opt} in (5) is converted to finding the best set of coefficients c_k 's for the basis functions. This can be done by substituting (10) into (5) and solving it using numerical optimization tools (e.g., Matlab *fmincon* function) under appropriate constraints, e.g., in the case $n = 3$, the constraints are given by (11) and (22) for piecewise linear and sine basis functions, respectively.

To demonstrate the proposed optimization methods, Figure 2 (a) shows the result of linear mapping ($S = 0.8853$), where the window width and window center parameters are preset values embedded in the DICOM header. Our optimization algorithm does not change these parameters, but attempts to find

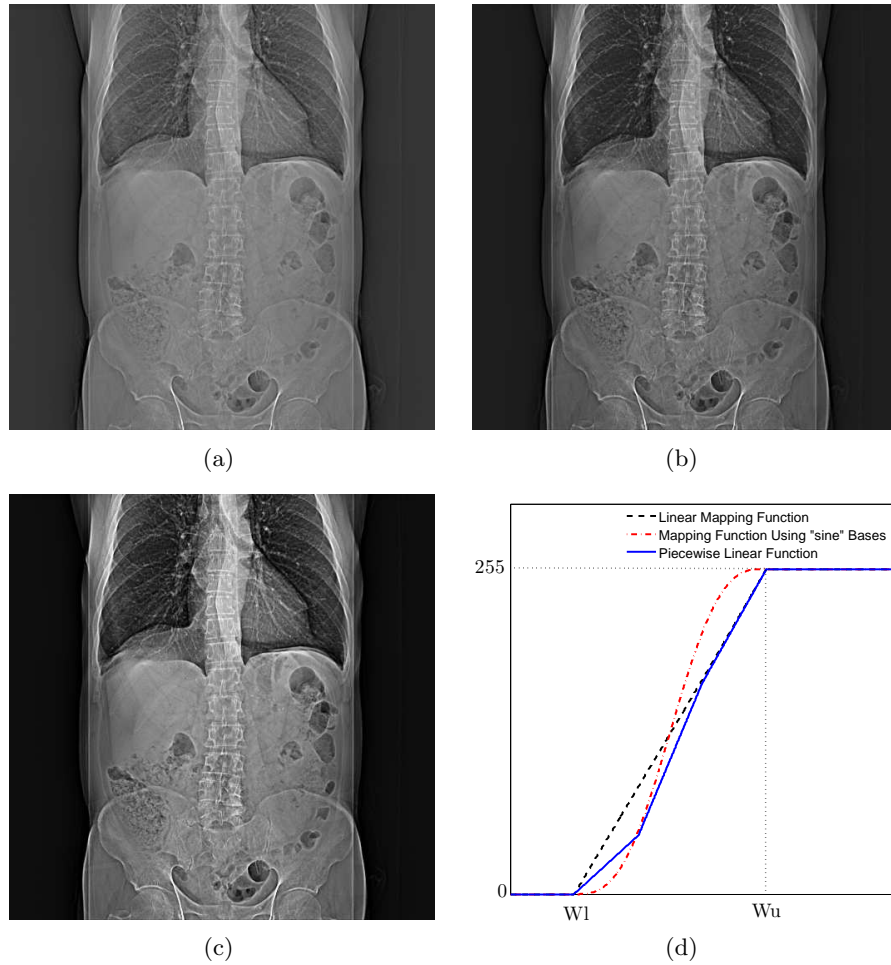


Fig. 2. Results of the optimization method. (a) with $S = 0.8853$ is the tone mapped image using linear mapping function where the window width and window center are read from DICOM file header. (b) with $S = 0.9292$ and (c) with $S = 0.9446$ are the enhanced images employing functions in (10) and (14), respectively. Image courtesy of AGFA Healthcare Inc.

the optimal values for c_1 and c_2 . Figure 2 (b) illustrates the result of optimal piecewise linear mapping, where the best coefficients are given by $c_1 = -0.15$ and $c_2 = -0.01$ and $S = 0.9294$ is obtained. Enhanced contrast in the image is observed, where the details in the spine and the lung are more discernable. Using the family of sine bases, Figure 2 (c) is obtained for optimal coefficients $c_1 = -0.0001$ and $c_2 = -0.16$ with even higher structural fidelity measure $S = 0.9446$, producing an image with higher contrast and more visible details.

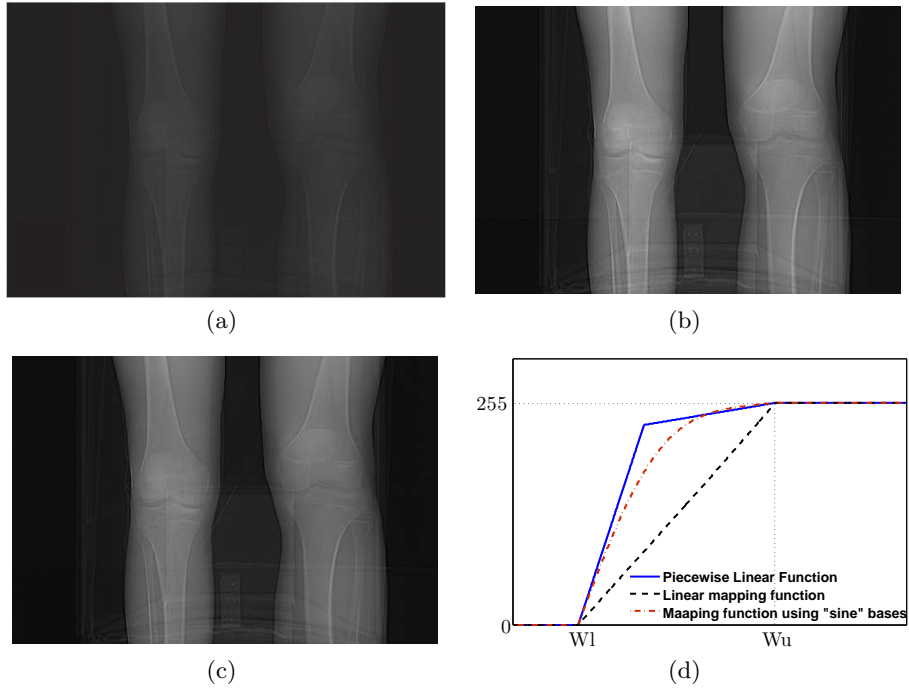


Fig. 3. Results of the optimization method for the bone. (a) with $S = 0.7746$ is the linearly mapped image using predefined windowing parameters for bone (window width = 2000, window center = 500). (b) with $S = 0.99$ and (c) with $S = 0.9852$ are the enhanced images using functions in (10) and (14), respectively. Image courtesy of AGFA Healthcare Inc.

As was mentioned before, the window width and the window center parameters in HDR file header do not necessarily provide a desirable contrast for specific body parts such as the lung, the bone, the soft tissue and the brain. In practice, radiologists often change them manually for different body parts in order to visualize the desired region with appropriate contrast. Figure 3 (a) is the tone mapped image using DICOM standard windowing procedure with predefined values for bone where $S = 0.7746$. The result of our optimization method using piecewise linear windowing is shown in Figure 3(b), where $c_1 = 0.56$, $c_2 = 0.28$ and $S = 0.99$. Figure 3 (c) shows the image produced by optimal sine basis windowing with coefficients $c_1 = 0.37$ and $c_2 = 0.04$ and quality measure $S = 0.9852$. It can be observed that the performance of the optimization task using either approaches provides images with strong contrast enhancement. The optimal windowing curve in Fig. 3 (d) reveals that the intensity of CT bone images is concentrated in the middle of the window width. Since piecewise linear functions can model drastically increasing functions, it works slightly better than the sine bases.

4 Conclusion and Future Work

In order to overcome the problem of displaying HDR medical images on standard LDR displays, a number of tone mapping algorithms that convert HDR to LDR images have been developed. Many of these methods employ a straightforward linear mapping from the window of interest to the low dynamic range. We have shown that such commonly used linear functions are unable to map structural information accurately and have proposed an optimization framework to construct superior windowing functions that enhance contrast. The optimization task seeks to maximize the structural fidelity measure in the tone-mapped LDR image using the HDR medical image as reference. Our experiments have demonstrated very promising results. In the future, there are some areas to be further explored. Specifically, other families of continuous and monotonically increasing functions should be examined. Clinically reliable subjective tests by radiologists should be carried out to evaluate and calibrate the structural fidelity measure.

References

1. Peter G. J. Barten. *Contrast sensitivity of the human eye and its effects on image quality*. SPIE Optical Engineering Press, Washington, 1999.
2. C. Cavaro-Menard, L. Zhang, and P. Le Callet. Diagnostic quality assessment of medical images: Challenges and trends. In *2010 2nd European Workshop on Visual Information Processing, EUVIP2010*, pages 277–284, 2010.
3. Pamela C. Cosman, Robert M. Gray, and Richard A. Olshen. Evaluating quality of compressed medical images: SNR, subjective rating, and diagnostic accuracy. *Proceedings of the IEEE*, 82(6):919–932, 1994.
4. D. Koff, P. Bak, P. Brownrigg, D. Hosseinzadeh, A. Khademi, A. Kiss, L. Lepanto, T. Michalak, H. Shulman, and A. Volkening. Pan-canadian evaluation of irreversible compression ratios (“lossy” compression) for development of national guidelines. *Journal of Digital Imaging*, 22(6):569–578, 2009.
5. E. Reinhard, G. Ward, S. Pattanaik, P. Debevec, W. Heidrich, and K. Myszkowski. *High Dynamic Range Imaging: Acquisition, Display, and Image-Based Lighting*. Morgan Kaufmann Publishers Inc., 2010.
6. Z. Wang, A. C. Bovik, H. R. Sheikh, and E. P. Simoncelli. Image quality assessment: From error visibility to structural similarity. *IEEE Trans. Image Proc.*, 13:35–44, 2004.
7. H. Yeganeh and Z. Wang. Objective assessment of tone mapping algorithms. In *Proc. IEEE Int. Conf. Image Proc.*, 2010.
8. H. Yeganeh and Z. Wang. Objective quality assessment of tone mapped images. *Submitted to IEEE Trans. Image Proc.*, 2011.
9. H. Yeganeh and Z. Wang. *Structural fidelity vs. naturalness - Objective assessment of tone mapped images*, volume 6753 LNCS of *Lecture Notes in Computer Science (including subseries Lecture Notes in Artificial Intelligence and Lecture Notes in Bioinformatics)*. 2011.